Self-Propelled Devices

Deutsche Ausgabe: DOI: 10.1002/ange.201505155
Internationale Ausgabe: DOI: 10.1002/anie.201505155

Micromotor-Based Biomimetic Carbon Dioxide Sequestration: Towards Mobile Microscrubbers

*Murat Uygun, Virendra V. Singh, Kevin Kaufmann, Deniz A. Uygun, Severina D. S. de Oliveira, and Joseph Wang**

***Abstract:** We describe a mobile CO_2 scrubbing platform that offers a greatly accelerated biomimetic sequestration based on a self-propelled carbonic anhydrase (CA) functionalized micromotor. The CO_2 hydration capability of CA is coupled with the rapid movement of catalytic micromotors, and along with the corresponding fluid dynamics, results in a highly efficient mobile CO_2 scrubbing microsystem. The continuous movement of CA and enhanced mass transport of the CO_2 substrate lead to significant improvements in the sequestration efficiency and speed over stationary immobilized or free CA platforms. This system is a promising approach to rapid and enhanced CO_2 sequestration platforms for addressing growing concerns over the buildup of greenhouse gas.*

Carbon dioxide emissions are considered to be one of the major contributions to climate change.[1–3] Considerable efforts aimed at mitigating the accumulations of CO_2 are currently underway. New approaches are thus being developed to capture and sequester CO_2, from effluents and the atmosphere, including adsorption on oxides,[4] zeolites,[5] metal–organic frameworks,[6] and ionic liquids.[7] Each of these CO_2 capture processes has its own disadvantages, such as high cost, high energy input, use of harsh chemicals, and generation of pollutants.[8] Storing the dissolved CO_2 (as solid calcium carbonate) is one of the most promising and environmentally reliable methods to reduce the amount of CO_2 dissolved in water samples.[9,10] In this case, the CO_2 is hydrated by water, followed by ionization and carbonate formation using calcium chloride.[11] The mechanism for such CO_2 sequestration involves the following steps:

$$CO_2(g) \leftrightarrow CO_2(aq) \tag{1}$$

$$CO_2(aq) + H_2O \leftrightarrow H_2CO_3(aq) \tag{2}$$

$$H_2CO_3 \leftrightarrow H^+ + HCO_3^- \tag{3}$$

$$HCO_3^- \leftrightarrow H^+ + CO_3^{2} \tag{4}$$

$$Ca^{2+} + CO_3^{2-} \rightarrow CaCO_3 \tag{5}$$

Here, the hydration of CO_2 is the rate-limiting step, which restricts the broad applicability of this methodology.[12] Recently, a biomimetic CO_2 sequestration route using carbonic anhydrase (CA) has demonstrated good efficiency toward CO_2 capture by catalyzing the CO_2 hydration rate.[13] Such a catalytic sequestration system offers several potential advantages over the above-mentioned sequestration techniques, including being a cost-effective, environmentally friendly, ambient-temperature process that is specific for CO_2, suitable for on-site operation, and does not require concentration and transportation steps.[13,14] CA is a zinc metalloenzyme that catalyzes the hydration of CO_2 to form bicarbonate.[15] The use of free CA for CO_2 mineralization is compromised by the limited enzyme stability and reusability,[16] which can be increased by immobilizing CA onto various solid supports.[16] However, such CA-loaded stationary platforms are characterized by low CO_2 sequestration efficiency and lengthy operation times.

Herein we describe a new approach based on CA-functionalized micromotors for greatly enhanced CO_2 sequestration. This approach combines the biocatalytic activity of CA with the self-propulsion of chemically powered micromotors through CO_2-saturated samples to act as highly efficient mobile biocatalytic microscrubbers. Recent advances in the field of synthetic nano/micromotors have expanded the performance, capabilities, and functionalities of these tiny vehicles.[17] These developments have opened up a breadth of applications in diverse fields, ranging from energy generation,[18] environmental cleanup,[19] or disease diagnosis[20] and treatment.[21] For example, various detoxification reactions[19] and sensing protocols[20] have been shown to be rapidly accelerated by the autonomous motion of catalytic micromotors and the enhanced fluid mixing generated by such movement.

The immobilization of enzymes on micromotor surfaces was first demonstrated in 2009 when catalase was used as a replacement for Pt to achieve motion.[22] For performing such effective "on-the-move" CO_2 sequestration, we utilized COOH-polypyrrole:poly(3,4-ethylenedioxythiophene)/Pt (COOH-PPy:PEDOT/Pt) tubular micromotors modified with the CA enzyme (Figure 1 A) to catalyze the slowest step of sequestration, that is, the hydration of CO_2 to bicarbonate, which can be mineralized as $CaCO_3$ (Figure 1 B,C). The resulting mobile CO_2 scrubbing platform leads to a dramatic increase in the CO_2 sequestration efficiency while greatly decreasing the reaction time because of the self-mixing and convection (induced by the micromotor movement). The autonomous motion of the micromotors also prevents their sedimentation. The hydrodynamics of the self-

---

[*] Dr. M. Uygun,[+] Dr. V. V. Singh,[+] K. Kaufmann, Dr. D. A. Uygun,
S. D. S. de Oliveira, Prof. J. Wang
Department of Nanoengineering
University of California, San Diego
La Jolla, CA 92093 (USA)
E-mail: josephwang@ucsd.edu

[+] These authors contributed equally to this work.

Supporting information for this article is available on the WWW under http://dx.doi.org/10.1002/anie.201505155.

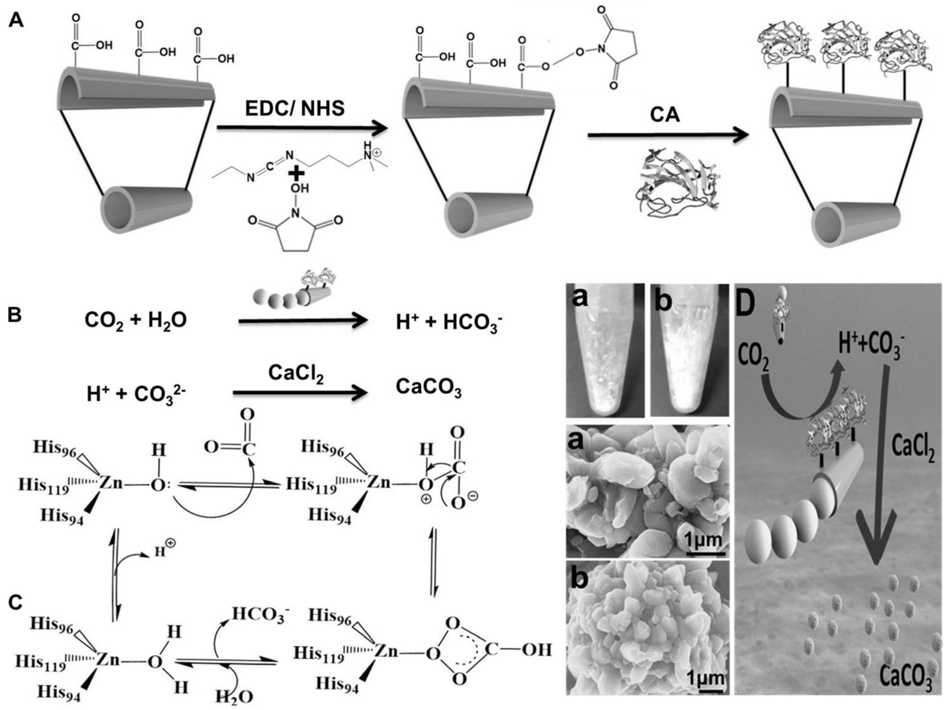

Figure 1. Micromotor-based CO_2 sequestration platform. A) Modification of the micromotor surface by EDC/NHS coupling followed by immobilization of CA. B, D) Micromotor-based CO_2 sequestration offering enhanced and rapid hydration to bicarbonate followed by precipitation using $CaCl_2$; (right) photographs of $CaCO_3$ precipitates after treatment with CA immobilized on static (a) and moving (b) micromotors. C) Mechanism of the CO_2 hydration catalyzed by CA; a, b) SEM images of the resulting $CaCO_3$ crystals. D) CO_2 scrubbing operation.

propelled CA-modified micromotor system thus enhances the biocatalytic CO_2 hydration process and provides attractive advantages over static enzyme systems. Figure 1 shows CA immobilization by the surface carboxylic groups of the outer layer along with the cross section of the microengine and the corresponding surface layers. The exposed surface carboxyl groups were activated using 1-ethyl-3-(3-dimethylaminopropyl)-carbodiimide/*N*-hydroxy succinimide (EDC/NHS) for conjugation with CA. The catalytic decomposition of the hydrogen peroxide fuel at the inner Pt layer of the micromotor generates the oxygen bubble thrust and leads to an efficient autonomous motion of the enzyme-modified microengine. Figure 1B shows the micromotor-based rapid "on-the-move" biocatalytic hydration of CO_2 to form a bicarbonate ion, followed by the precipitation of $CaCO_3$ in the presence of $CaCl_2$, along with images of the $CaCO_3$ precipitate using the static and moving CA-immobilized micromotor (Figure 1B, a and b, respectively). The enzyme CA is able to accelerate the interconversion of CO_2 to bicarbonate, as shown in Figure 1C, leading to significantly higher amounts of $CaCO_3$ (Figure 1B). Scanning electron microscopy (SEM) images of the formed $CaCO_3$ showed rhombohedral and rectangle-shaped crystals, thus confirming that the crystals formed are calcite and vaterite particles (Figure 1C, a and b) as reported elsewhere.[23]

Figure 2A and B show SEM images and energy-dispersive spectroscopic (EDX) mapping of the 6 µm long unmodified and modified micromotors, respectively. The EDX study was carried out in order to confirm the CA immobilization based on the presence and absence of Zn^{2+} for the modified and unmodified motors, respectively (Figure 2A, B). Figure 2C shows time-lapse images, taken from videos in the Supporting Information, illustrating the fast movement of the enzyme-immobilized micromotors in untreated sea water. The CA-modified micromotors undergo efficient propulsion at high speeds (e.g., 106 µm s^{-1} using 2% peroxide), with curved, circular, and self-rotating trajectories, consistent with previous reports.[24b] As expected, the speed of the functionalized micromotors is strongly dependent on the concentration of the peroxide fuel, and increases from 106 to 198 and 284 µm s^{-1} using 2, 3, and 4% fuel concentrations, respectively ($n=$ 50 micromotors). Note that the unmodified motors display even higher speeds (e.g., 197 µm s^{-1} using 2% peroxide; Figure S1A in the Supporting Information). We have tested the micromotors in additional media (e.g., lake water) and observed no alteration in their movement, in agreement with earlier reports.[24a,b]

Before proceeding to study the CO_2 sequestration efficiency of micromotors, it was very important to estimate how much CA was immobilized onto the micromotor in order to compare the CO_2 sequestration efficiency with that of the free enzyme. A spectrophotometric calibration curve, used to deduce the amount of immobilized enzyme (Figure S1B), indicated the presence of 586 µg CA on 3×10^6 micromotors.

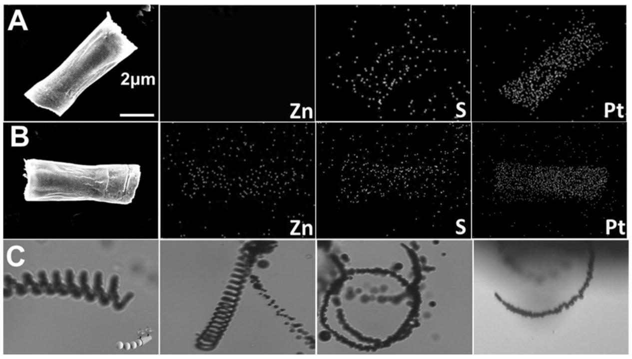

Figure 2. SEM and EDX images showing the different micromotors: A) unmodified micromotor; B) CA-functionalized micromotor; the presence of Zn confirms the enzyme immobilization. C) Video frames showing the different trajectories of the modified micromotor in seawater. Conditions: 2% H_2O_2 and 1% sodium cholate.

Two separate studies examining the influence of the peroxide fuel and surfactant upon the CA activity indicated that relevant levels of these constituents have a negligible effect upon the enzymatic activity (Figures S2 and S3).

The self-propulsion capability of the functionalized micromotors, along with the corresponding bubble tail, leads to a favorable hydrodynamic environment that increases the rate of the biocatalytic reaction between the CA-modified micromotors and the CO_2-saturated solution (without external stirring), thereby offering a rapid CO_2 scrubbing platform. As shown in Figure 3F, the mobile modified micromotors result in a high yield of $CaCO_3$, corresponding to a 90% efficiency within 5 min. The driving force for this high sequestration efficiency is the mixing and convection induced by the micromotor motion, which enhances mass transport of the CO_2 substrate, and, along with the continuous motion of the enzyme, leads to a faster rate of the enzymatic hydration of CO_2. The potential of the micromotor-based CO_2 sequestration was also examined in sea water and resulted in a similar (88%) efficiency (Figure 3G). In contrast, dramatically lower CO_2 sequestration efficiencies of 0, 2.4, 7.8, 9.8, and 31.0% were observed in control experiments involving unmodified micromotors (Figure 3A), modified micromotors with denatured CA (Figure 3B), static CA-functionalized micromotors (Figure 3C), the static free enzyme (Figure 3D), and modified micromotors without the surfactant sodium cholate (Figure 3E), respectively (Table S1). The micromotor biocatalytic process thus leads to 9.2- and 11.5-fold enhancements of the sequestration efficiency compared to the static free and immobilized CA, respectively. In the case of denatured enzyme micromotors, minimal CO_2 sequestration can be attributed to the loss of enzymatic activity after heating CA above 90 °C.[25] The low reaction efficiency in the presence of the static CA-modified micromotors and the stationary free enzyme reflects the diffusion-limited process that hinders the efficient utilization of the enzyme.

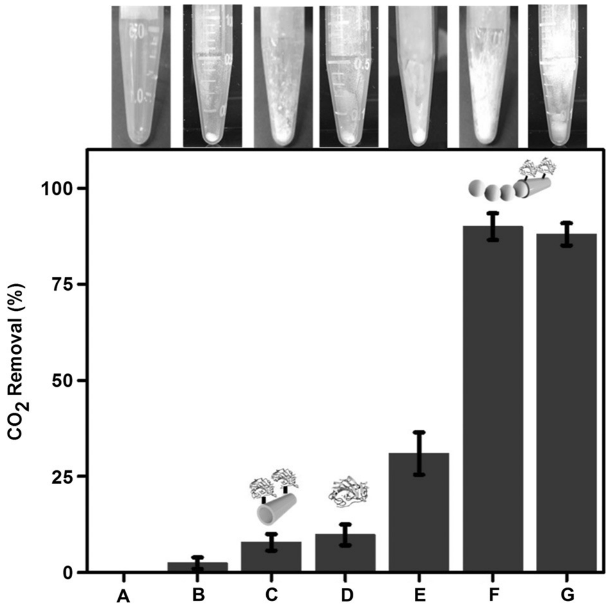

Figure 3. Micromotor-based CO_2 sequestration and control experiments. CO_2 sequestration efficiency in the presence of A) unmodified motor, B) modified motor with denaturated CA, C) static CA-modified motors, D) the static free CA; E) CA modified motors without sodium cholate. F,G) CA-modified motors in pure water and in sea water, respectively. Top: corresponding images of the $CaCO_3$ precipitate. Reaction conditions: 2 mL CO_2-saturated solution, 4×10^6 micromotors, 2% H_2O_2, and 1% sodium cholate for 5 min, followed by a 5 min reaction with 5% $CaCl_2$ (2 mL). Error bars represent the standard deviation ($n=5$).

The greatly enhanced CO_2 sequestration ability of the micromotors is associated with their continuous movement and thus depends upon several interdependent parameters. A detailed characterization study, examining the effect of the number of micromotors, peroxide concentration, pH value, and the sequestration time upon the sequestration efficiency, was carried out for selecting the optimal working conditions (Figure 4). For example, Figure 4A shows the effect of the number of micromotors, between 1×10^6–5×10^6 micromotors/mL, on the sequestration efficiency with a 5 min propulsion time in 2 mL of CO_2-saturated solution. The efficiency increased in a nearly linear fashion from around 24% for 1×10^6 micromotors to nearly 90% for 4×10^6 micromotors. As expected, increasing the level of the peroxide fuel from 0.5 to 1.5% resulted in a dramatic increase in the sequestration efficiency from 12 to 80% (Figure 4B), thus reflecting the significantly higher motor speed and corresponding fluid transport at high fuel levels. The influence of the solution pH value is shown in Figure 4C. The efficiency increases rapidly from 15% to around 85% upon raising the pH value from 2 to 6, and remained nearly constant thereafter, as expected from the optimal pH value of 7.2 for the CA activity.[26] Figure 4D shows the influence of the micromotor movement time upon the sequestration efficiency. The efficiency initially increases rapidly with the reaction time (within 3 min), and approaches approximately 90% sequestration over a 5 min period.

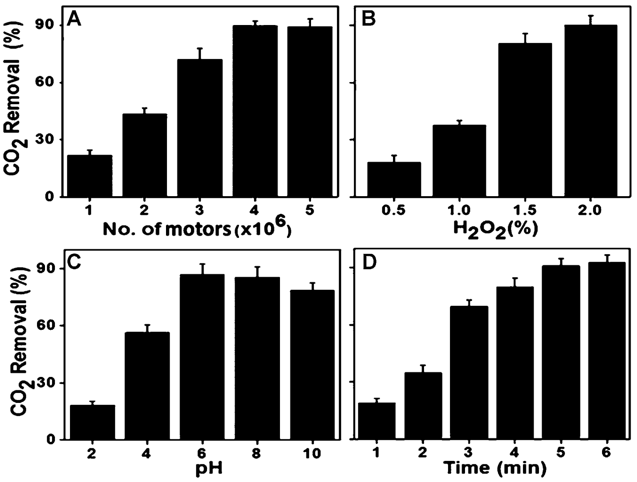

Figure 4. Factors affecting the efficiency of the micromotor-based CO_2 sequestration. Effect of the A) number of micromotors, B) peroxide concentration, C) pH, and D) motor navigation time. Peroxide concentration (A,C,D), 2%; amount of micromotors (B,C,D), 4×10^6 micromotors/mL; navigation time (A–C), 5 min. Motor counts were performed by averaging the number of motors per 1 µL aliquots ($n=10$). Error bars represent the standard deviation ($n=10$).

The potential of these functionalized micromotors for environmental applications was further studied by investigating the extent of CA leaching and their thermal or storage stability. The covalent attachment of the enzyme to the micromotors means that it is strongly adsorbed and thus any potential leaching is minimized. Figure S1C shows the stability of the free and immobilized CA after storage. The modified micromotors retained their biocatalytic activity over long periods (e.g., 77% of the initial activity after 30 days storage at 4°C), in agreement with earlier reports on immobilized CA.[27] In contrast, the free CA retained only 36% of its original activity over the same period. Similarly, and as expected,[28] the enzyme immobilized on the micromotor shows high thermal stability compared to the free enzyme. Figure S1D shows the heat inactivation curve of the immobilized and free enzymes at different incubation temperatures. Even at 60°C, which is reported as the thermal denaturation temperature of free CA,[28] the immobilized enzyme retained 68% of its stability over a 30 min period, compared to only 37% for the free enzyme. The increased stability of CA immobilized on solid supports has been reported previously and is attributed to the minimization of conformational changes.[28] If necessary, biomimetic artificial enzymes[29] could also be considered for stability enhancement.

In conclusion, we have described a mobile CO_2-scrubbing platform that couples the biocatalytic activity of CA with the autonomous movement of chemically powered micromotors to offer highly efficient and rapid CO_2 sequestration. The self-propelled CA-functionalized micromotors are shown to accelerate the hydration of CO_2 because of dramatically enhanced fluid transport and continuous movement of CA. These factors result in significant improvements in the CO_2 sequestration efficiency and reaction time. The practical utility of the new biomimetic micromotor approach has been demonstrated in seawater. This system is attractive for remote field conditions or in situ sequestration of natural water (where mechanical agitation is not feasible) and can be scaled up. While the present proof-of-concept study has utilized peroxide-driven micromotors, this “on-the-move” sequestration concept could be realized by using different motor systems. These include recently introduced water-based micromotors, powered by natural aqueous media (acting as an in situ fuel),[30] that obviate the need for H_2O_2 or expensive Pt catalysts. Other modern micromotors, such as biocatalytic (catalase) micromotors or fuel-free ultrasound motors, could be used to reduce costs, eliminate external fuels, and increase the scale on which these microscrubbers could be employed. Our research group is currently developing macroscale motors that cover large areas (meters), towards large-scale CO_2 scrubbing. This enzymatic CO_2 sequestration strategy thus represents a promising route to mitigate the buildup of a major greenhouse gas in the environment and is expected to pave the way for diverse applications.

Acknowledgements

M.U. and D.A.U acknowledge a fellowship from The Scientific and Technological Research Council of Turkey (TUBITAK). S.D.S.de O. acknowledges a fellowship from the Brazilian Ministry of Education. We would like to acknowledge F. Soto for his assistance.

Keywords: carbon dioxide · carbonic anhydrase · enzymes · greenhouse gases · micromotors

How to cite: *Angew. Chem. Int. Ed.* **2015**, *54*, 12900–12904
Angew. Chem. **2015**, *127*, 13092–13096

---

[1] G. Bhattacharjee, A. Kumar, T. Sakpal, R. Kumar, *ACS Sustainable Chem. Eng.* **2015**, *3*, 1205.

[2] R. Kumar, P. Linga, J. A. Ripmeester, P. J. Englezos, *Environ. Eng.* **2009**, *135*, 411.

[3] D. A. Lashof, D. R. Ahuja, *Nature* **1990**, *344*, 529.

[4] K. B. Lee, M. G. Beaver, H. S. Caram, S. Sircar, *Ind. Eng. Chem. Res.* **2008**, *47*, 8048.

[5] S. Cavenati, C. A. Grande, A. E. Rodrigues, *J. Chem. Eng. Data* **2004**, *49*, 1095.

[6] P. L. Llewellyn, S. Bourrelly, C. Serre, Y. Filinchuk, G. Ferey, *Angew. Chem. Int. Ed.* **2006**, *45*, 7751; *Angew. Chem.* **2006**, *118*, 7915.

[7] M. Ramdin, T. W. de Loos, T. J. H. Vlugt, *Ind. Eng. Chem. Res.* **2012**, *51*, 8149.

[8] M. M. Abu-Khader, *Energy Sources Part A* **2006**, *28*, 1261.

[9] T. R. Karl, K. E. Trenberth, *Science* **2003**, *302*, 1719.

[10] S. Lee, D. H. Sin, K. Cho, *Cryst. Growth Des.* **2015**, *15*, 610.

[11] F. R. Keene in *Electrochemical and Electrocatalytic Reactions of Carbon Dioxide* (Eds.: B. P. Sullivan, K. Krist, H. E. Guard), Elsevier, Amsterdam, **1993**, pp. 1–18.

[12] G. A. Bhaduri, L. Siller, *Catal. Sci. Technol.* **2013**, *3*, 1234.

[13] a) M. Vinoba, D. H. Kim, K. S. Lim, S. K. Jeong, S. W. Lee, M. Alagar, *Energy Fuels* **2011**, *25*, 438; b) G. M. Bond, J. Stringer, D. K. Brandvold, F. A. Simsek, M. G. Medina, G. Egeland, *Energy Fuels* **2001**, *15*, 309; c) S. Bhattacharya, A. Nayak, M. Schiavone, S. K. Bhattacharya, *Biotechnol. Bioeng.* **2004**, *86*, 37.

[14] R. Baciocchi, A. Polettini, R. Pomi, V. Prigiobbe, V. N. Von Zedwitz, A. Steinfeld, *Energy Fuels* **2006**, *20*, 1933.

[15] V. M. Cangelosi, A. Deb, J. E. Penner-Hahn, V. L. Pecoraro, *Angew. Chem. Int. Ed.* **2014**, *53*, 7900; *Angew. Chem.* **2014**, *126*, 8034.

[16] a) D. M. D’Alessandro, B. Smit, J. R. Long, *Angew. Chem. Int. Ed.* **2010**, *49*, 6058; *Angew. Chem.* **2010**, *122*, 6194; b) B. H. Jo, J. H. Seo, Y. Y. Yang, K. Baek, Y. S. Choi, S. P. Pack, S. H. Oh, H. J. Cha, *ACS Catal.* **2014**, *4*, 4332.

[17] a) J. Wang, *Nanomachines: Fundamentals and Applications*, Wiley, Hoboken, **2013**; b) W. F. Paxton, S. Sundararajan, T. E. Mallouk, A. Sen, *Angew. Chem. Int. Ed.* **2006**, *45*, 5420; *Angew. Chem.* **2006**, *118*, 5546; c) S. Sánchez, L. Soler, J. Katuri, *Angew. Chem. Int. Ed.* **2015**, *54*, 1414; *Angew. Chem.* **2015**, *127*, 1432; d) J. G. S. Moo, M. Pumera, *Chem. Eur. J.* **2015**, *21*, 58; e) M. Guix, C. C. Mayorga-Martinez, A. Merkoci, *Chem. Rev.* **2014**, *114*, 6285.

[18] V. V. Singh, F. Soto, K. Kaufmann, J. Wang, *Angew. Chem. Int. Ed.* **2015**, *54*, 6896; *Angew. Chem.* **2015**, *127*, 7000.

[19] a) J. Wang, W. Gao, *ACS Nano* **2014**, *8*, 3170; b) L. Soler, V. Magdanz, V. M. Formin, S. Sanchez, O. G. Schmidt, *ACS Nano* **2013**, *7*, 9611; c) L. Soler, S. Sanchez, *Nanoscale* **2014**, *6*, 7175; d) V. V. Singh, B. Jurado-Sanchez, S. Sattayasamitsathit, J. Orozco, J. Li, M. Galarnyk, Y. Fedorak, J. Wang, *Adv. Funct. Mater.* **2015**, *25*, 2147; e) J. Li, V. V. Singh, S. Sattayasamitsathit,

J. Orozco, K. Kaufmann, R. Dong, W. Gao, B. Jurado-Sanchez, Y. Fedorak, J. Wang, *ACS Nano* **2014**, *8*, 11118; f) J. Orozco, B. Jurado-Sanches, G. Wagner, W. Gao, R. Vazquez-Duhalt, S. Sattayasamitsathit, M. Galarnyk, A. Cortes, D. Saintillan, J. Wang, *Langmuir* **2014**, *30*, 5082.

[20] a) J. Wang, W. Gao, *ACS Nano* **2012**, *6*, 5745; b) D. J. Irwin, *Nat. Mater.* **2011**, *10*, 342; c) B. J. Nelson, I. K. Kaliakatsos, J. J. Abbott, *Annu. Rev. Biomed. Eng.* **2010**, *12*, 55; d) S. Campuzano, J. Orozco, D. Kagan, M. Guix, W. Gao, S. Sattayasamitsathit, J. C. Claussen, A. Merkoci, J. Wang, *Nano Lett.* **2012**, *12*, 396; e) E. Morales-Narváez, M. Guix, M. Medina-Sánchez, C. Mayorga-Martinez, A. Merkoçi, *Small* **2014**, *10*, 2542; f) X. Yu, Y. Li, J. Wu, H. Ju, *Anal. Chem.* **2014**, *86*, 4501.

[21] a) R. Mhanna, F. Qiu, L. Zhang, Y. Ding, K. Sugihara, M. Zenobi-Wong, B. J. Nelson, *Small* **2014**, *10*, 1953; b) A. A. Solovev, W. Xi, D. H. Gracias, S. M. Harazim, C. Deneke, S. Sanchez, O. G. Schmidt, *ACS Nano* **2012**, *6*, 1751; c) Y. F. Mei, G. S. Huang, A. A. Solovev, E. B. Urena, I. Monch, F. Ding, T. Reindl, R. K. Y. Fu, P. K. Chu, O. G. Schmidt, *Adv. Mater.* **2008**, *20*, 4085; d) Z. Wu, Y. Wu, W. He, X. Lin, J. Sun, Q. He, *Angew. Chem. Int. Ed.* **2013**, *52*, 7000; *Angew. Chem.* **2013**, *125*, 7138.

[22] S. Sanchez, A. A. Solovev, Y. Mei, O. G. Schmidt, *J. Am. Chem. Soc.* **2010**, *132*, 13144.

[23] N. Favre, M. L. Christ, C. P. Pierre, *J. Mol. Catal. B* **2009**, *60*, 163.

[24] a) W. Gao, S. Sattayasamitsathit, J. Orozco, J. Wang, *Nanoscale* **2013**, *5*, 8909; b) G. Zhao, H. Wang, B. Khezri, R. D. Webster, M. Pumera, *Lab Chip* **2013**, *13*, 2937; c) A. Solovev, Y. Mei, E. Bermudez, G. Huang, O. Schmidt, *Small* **2009**, *5*, 1688.

[25] M. Amani, R. Khodarahmi, S. Ghobadi, M. Mehrabi, B. I. Kurganov, A. A. Moosavi-Movahedi, *J. Chem. Eng. Data* **2011**, *56*, 1158.

[26] S. Wanjari, C. Prabhu, R. Yadav, T. Satyanarayana, N. Labhsetwar, S. Rayalu, *Process Biochem.* **2011**, *46*, 1010.

[27] M. Vinoba, M. Bhagiyalakshmi, S. K. Jeong, Y. I. Yoon, S. C. Nam, *J. Phys. Chem. C* **2011**, *115*, 20209.

[28] a) G. Merle, S. Fradette, E. Madore, J. E. Barralet, *Langmuir* **2014**, *30*, 6915; b) E. Ozdemir, *Energy Fuels* **2009**, *23*, 5725.

[29] J. G. S. Moo, H. Wang, G. Zhao, M. Pumera, *Chem. Eur. J.* **2014**, *20*, 4292.

[30] W. Gao, X. Feng, A. Pei, Y. Gu, J. Li, J. Wang, *Nanoscale* **2013**, *5*, 4696.

Received: June 10, 2015
Revised: August 24, 2015